MATERIALS PHYSICS AND MECHANICS RESEARCH ARTICLE

Submitted: July 4, 2025 Revised: November 26, 2025 Accepted: Murch 10, 2026

CFD evaluation of the hydrodynamic and thermal performances of a counter-flow heat exchanger

R. Nebbati [1] ✉, **M. Kadja** [1], **F. Mechighel** [2]

[1] University of Brothers Mentouri Constantine 1, Constantine, Algeria

[2] Badji Mokhtar University – Annaba, Annaba, Algeria

✉ nebbatirabah@yahoo.com

ABSTRACT

A heat exchanger is a device that facilitates the transfer of energy between two fluids through a solid barrier. Simulations were performed in a turbulent flow regime to investigate the two-dimensional forced convective heat transfer of the nanofluid water / Al_2O_3 within a counter-flow heat exchanger. This study is numerical and was conducted using a single-phase approach with constant thermophysical properties. Conduction through the interface was taken into account in the computations. The results unequivocally showed an improvement in the overall coefficient of heat transfer depending on the Reynolds number along with the type of fluid. The use of nanofluid significantly increases total heat transfer in contrast to the pure base fluid; however, this is accompanied by an increase in friction coefficients, leading to higher pumping costs.

KEYWORDS

computational fluid dynamics • fully developed turbulent flow • double tube heat exchanger numerical convective heat transfer • overall heat transfer coefficient

Citation: Nebbati R, Kadja M, Mechighel F. CFD evaluation of the hydrodynamic and thermal performances of a counter-flow heat exchanger. *Materials Physics and Mechanics*. 2026;54(2): 167–180. http://dx.doi.org/10.18149/MPM.5422026_12

Introduction

The thermal energy exchanger is one of the key instruments of the thermal engineer or energy engineer, whether its goal is the manufacture of a product whose development passes through a set of cycles where temperature and pressure vary [1], or whether it involves the production of mechanical (or electrical) energy from thermal energy [2]. Essentially, a hot fluid circulates from an inlet of the exchanger to its outlet by transferring part of its enthalpy to a cold fluid which also circulates between an inlet and an outlet distinct from those of the hot fluid.

Heat exchangers are mainly used in various industrial sectors, including chemicals, petrochemicals, steel, agri-food, and energy production, along with transportation (automobile, aeronautics) and residential and tertiary sectors (heating, air conditioning, etc.) [3,4]. The selection of a heat exchanger for any application is influenced by numerous factors: the temperature and pressure ranges of the fluids, their physical characteristics and corrosiveness, maintenance considerations, and size. It is evident that a well-suited, correctly sized, robust, and efficiently operated exchanger contributes to improved process efficiency and energy utilization [5]. Due to their importance in industry many recent studies have been published by researchers, whether theoretical or numerical, on these devices. In the work of Pathak et al. [6], a concentric pipe counterflow heat

Publisher: Peter the Great St. Petersburg Polytechnic University

exchanger (CPCFHEx) is examined to enhance its performance under various conditions. Velocity, pressure, temperature, and turbulence profiles are analyzed in pipes using the CFD (computational fluid dynamics) simulation method. The analysis encompasses pressure drops, velocity variations, total heat transfer coefficients, and effectiveness for CPCFHEx. The study includes an examination of entropy, exergy, and entransy across various flow rates and internal pipe materials to identify the best operating conditions. Following the analysis, the results indicate that copper achieves a maximum temperature difference of 4.688 K and an effectiveness of 0.1562 for the cold fluid at low flow rates (0.081 and 0.19 kg/s). On the other hand, steel shows a maximum temperature difference of 1.595 K for the hot fluid at higher flow rates (0.1 and 0.22 kg/s). The analysis reveals that at high flow rates, copper achieves a maximum heat transfer rate of 1.603 W and a total heat transfer coefficient of 3.160 W/m^2 K, alongside maximum entropy generation rates of 1.144 J/s and exergy destruction at 343.2 J/s. Conversely, steel displays a minimum entransy dissipation rate of 19874.925 JK/s and an entransy dissipation number of 0.4516 at these flow rates. To achieve better heat exchanger performance in terms of rate heat transfer, effectiveness, entropy generation, as well as exergy destruction, selecting high-conductivity materials for the pipes and maintaining low fluid flow rates is advisable.

Incorporating nanoparticles into traditional heat transfer fluids enhances the thermal properties and stability of the suspension was proposed by Choi and Eastman [7] in 1995. Maryam Mousavi et al. [8] experimentally investigated the effect of singular, binary hybrid and ternary hybrid nanofuids including (water / CuO, water / $CaCO_3$ and water / SiO_2) on fully developed convective heat transfer and pressure loss in circular tube. The findings indicated a notable improvement in heat transfer rate and a significant decrease in pressure drop.

Ali et al. [9] investigated the efficiency of double pipe heat exchangers using different materials. The heat exchanger harnesses heat from steam waste recovery in a refinery process. Design of the double pipe heat exchangers is carried out using CATIA and GAMBIT, while CFD analysis is performed with ANSYS Fluent. Results are derived using three different materials: copper, steel, and aluminum. Parallel and counter-current flow heat exchangers were also numerically investigated by Dhoria et al. [10]. It was utilized ANSYS FLUENT 17.1 software, alongside theoretical calculations, to assess temperature drops in relation to inlet velocity as well as inlet temperature, investigating their variations. Design and simulation encompassed both parallel flow as well as counterflow heat exchanger models. Calculated outlet temperatures for parallel and counterflow heat exchangers, based on the inlet velocity and inlet temperature of the fluid medium, were utilized to determine the total coefficient of heat transfer. Values obtained after experiments on the heat exchanger setup for parallel and counterflow heat transfer are used for theoretical calculations. In the study of Ahmed et al. [11], CFD analysis was performed on parallel, counterflow shell-and-tube heat exchangers. The research explored multiple factors, including temperature, turbulence, kinetic energy, pressure drop, velocity, and the length of the heat exchanger's length was considered, with hot water flowing through the tube side and cold water through the shell side. As the cold water traveled along the shell side, its temperature gradually increased. Conversely, the temperature of the hot water on the tube area reduced along the length of the tube. This effect was more pronounced in the counterflow configuration compared to the parallel flow. Additionally, the velocity on the

shell side exhibited greater fluctuations due to the presence of baffles. As a result, pressure loss was higher in the cold water at the shell side than in the hot water at the tube side. To assess the impact of turbulence, turbulence kinetic energy was measured. Turbulence decreased in the initial section of the shell-and-tube heat exchangers, whereas it increased in the subsequent sections. All these observations and results were evaluated and subsequently analyzed. In the same year, Rabienataj Darzi et al. [12] also investigated the hydrodynamic and thermal characteristics of double-pipe heat exchangers (DPHEs). This experimental study aimed to explore the effects of an Al_2O_3 nanofluid with an average particle diameter of 20 nm on heat transfer, pressure drop, and thermal performance in a double pipe heat exchanger. The experiments were conducted for Reynolds numbers ranging from approximately 5,000 to 20,000 and for nanoparticle concentrations up to 1 % by volume. The results indicated that adding nanoparticles within the studied ranges has significant potential to enhance the thermal performance of the heat exchanger without causing a substantial increase in pressure drop. Ebrahim Tavousi et al. [13] provided a critical analysis of the impact of various passive methods on improving heat transfer rates, fluid flow characteristics, and friction factor enhancement in double-pipe heat exchangers. These methods included the use of turbulator inserts, extended surfaces (fins), changes in tube geometry, nanofluids, and combinations of these techniques. They concluded that combining turbulator inserts with nanofluids is the most effective approach for increasing heat transfer rates. Some researchers focused on modifying geometry and inserting elements into the inner and outer tubes [14,15]. Chun et al. [16] investigated the convective heat transfer coefficient of oil/alumina nanofluids in different volume fractions in a double pipe heat exchanger under laminar regime. They reported that the reason of heat transfer enhancement of nanofluids is the concentration of nanoparticles in thermal boundary layer near walls and particles motion. Dariush Mansourya et al. [17] experimentally studied a shell & tube heat exchanger and a plate heat exchanger under turbulent flow conditions using distilled water and water / Al_2O_3 nanofluid with 0.2, 0.5, and 1 % particle volume concentrations. Their results show, the double pipe heat exchanger revealed the best outcome for the heat transfer coefficient with a maximum enhancement of 60 % while a maximum enhancement in the heat transfer coefficient of 11 % was reported for the plate heat exchanger. Utilizing a nanofluid represented the lowest penalty in the pressure drop with a maximum enhancement of 27 % for the plate heat exchanger while the highest penalty in the pressure drop with a maximum enhancement of 85 % was observed in the double pipe and shell and tube heat.

The convective heat transfer performance and the flow characteristics of water / Al_2O_3 nanofluid flowing in heat exchangers, namely parallel flow, counter flow and shell and tube heat exchangers, have been experimentally investigated under laminar flow conditions by R. Dharmalingam et al. [18]. The effect of Al_2O_3 nanoparticle and the Reynolds number on the heat transfer performance and flow behavior of the nanofluid and water have been compared. It is concluded that for R_e = 1200, the ratio of overall heat transfer coefficient of water / Al_2O_3 nanofluid with that of water is 1.161 for parallel flow, 1.146 for counter flow, 1.171 for shell and tube heat exchangers. Zarringhalam et al. [19] experimentally investigated the convection heat transfer coefficient of water / CuO nanofluid with different volume fractions of turbulent flow through a counter flow double pipe heat exchanger. They figured out that by increasing

Reynolds number and volume fraction of nanoparticles to 2 %, the convection heat transfer enhances to 57 %.

Others investigated different fin shapes, while some explored the use of various working fluids, such as nanofluids [16,20]. In their study, Bouazizi and Turki [21]. numerically investigated forced convection flows in a horizontal channel through a porous medium. The results showed that in the absence of Brownian motion, the mean Nusselt number increases as the nanoparticle volume fraction φ increases. Investigation of gas dynamics in a heat exchanger turbulator with and without a lattice structure was examined numerically by Pulin et al. [22]. It was shown that the use of turbulators not only increases the efficiency of heat exchange processes, but also their resistance.

This study focuses on modeling a double-tube heat exchanger that operates with counter-flow, in which the fluids enter from opposite ends of the exchanger, with opposite flow directions, and exit the device through opposite ends.

Mathematical formulation

Geometric analysis and equation formulation

The investigated heat exchange challenge consists of circulating two fluids through conduits, which bring them into thermal contact. The illustrative schematic of the domain investigation is shown in Fig. 1, which shows that the two fluids are brought into thermal contact through a metallic wall, which promotes heat exchange. We have hot fluid, which transfers heat to cold fluid. The two fluids exchange heat through the wall. The inner pipe diameter of 15 mm has a thickness of 2 mm while the outer pipe diameter is 32 mm. Both pipes have a length of 1000 mm. The double tube heat exchanger is made of high heat conductive copper.

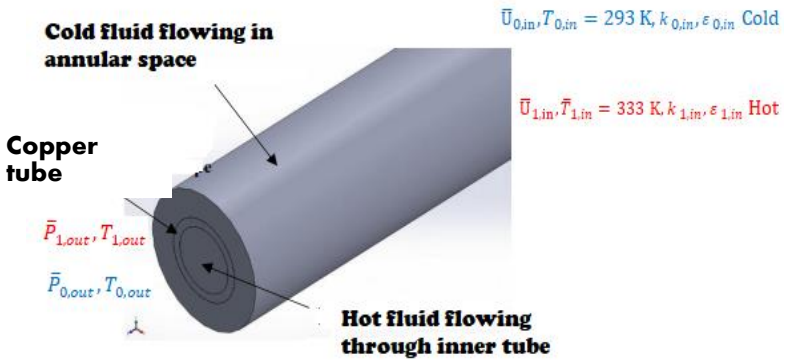

Fig. 1. Approached view of the double tube heat exchanger studied

The quantity of heat transferred depends on the exchange surface between the two fluids, but also on many other parameters, which makes a precise study of these devices quite complex [23]. Heat transfer is determined by the inlet temperature, the thermal characteristics of the fluids (including specific heat, thermal conductivity, dynamic viscosity, etc.), and the convection exchange coefficients (Table 1).

Table 1. The properties of the fluids and the material used

Fluide	Hot water at 333 K	Cold water at 293 K	Nano-fluid water / Al_2O_3 (φ = 3 %)	Copper
Density ρ, kg/m³	982.9	998.3	1086.9	8978
Specific heat C_p, JK/kg	4183	4181	3804.78	381
Thermal conductivity, W/mK	0.65	0.60	0.653	387.6
Dynamic viscosity, kgs/m	0.000472	0.00101	0.00113	-

This study assumed that the nanofluid possessed a uniform and stable composition, was incompressible, and maintained constant thermo-physical properties. The solid walls are made of copper with thermo-physical properties constants. Assuming the flow to be turbulent and steady with forced convection, the problem was analyzed in a 2D cylindrical coordinate system. Under these conditions, the modelled equations are presented in vector format as shown below:

1. conservation of mass $\frac{\partial \bar{U}_i}{\partial x_i} = 0,$ (1)

2. conservation of momentum $\bar{U}_j \frac{\partial \bar{U}_j}{\partial x_i} = -\frac{1}{\rho_{\mathrm{nf}}} \frac{\partial \overline{P'}}{\partial x_i} + \frac{\partial}{\partial x_j}\left(\left(\nu_{nf} + \nu_t\right)\frac{\partial \bar{U}_j}{\partial x_i}\right),$ (2)

where $\bar{P}' = \bar{P} - \frac{2}{3}\rho_{\mathrm{nf}} \cdot k,$

3. conservation of energy $\bar{U}_J \frac{\partial \bar{T}}{\partial x_j} = \frac{\partial}{\partial x_j}\left(\left(\frac{\nu_{nf}}{Pr_{nf}} + \frac{\nu_t}{Pr_t}\right)\frac{\partial \bar{T}}{\partial x_j}\right).$ (3)

Given that the nanofluid was considered a single-phase homogeneous fluid, the $k-\varepsilon$ turbulent model developed by [24] was used to define the turbulent viscosity, $\mu_t = \left(\rho C_\mu k^2\right)/\varepsilon$, through both additional equations for turbulent kinetic energy (k) and its dissipation rate (ε). These equations are formulated as follows:

$$\bar{U}_J \frac{\partial k}{\partial x_j} = \nu_t \left(\frac{\partial \overline{U_i}}{\partial x_j} + \frac{\partial \overline{U_J}}{\partial x_i}\right)\frac{\partial \overline{U_i}}{\partial x_j} + \frac{\partial}{\partial x_j}\left(\left(\nu_{nf} + \frac{\nu_t}{Pr_k}\right)\frac{\partial \kappa}{\partial x_j}\right) - \varepsilon, \quad (4)$$

$$\bar{U}_J \frac{\partial \varepsilon}{\partial x_j} = \nu_t C_{\varepsilon 1} \frac{\varepsilon}{k}\left(\frac{\partial \overline{U_i}}{\partial x_j} + \frac{\partial \overline{U_J}}{\partial x_i}\right)\frac{\partial \overline{U_i}}{\partial x_j} + \frac{\partial}{\partial x_j}\left(\left(\nu_{nf} + \frac{\nu_t}{Pr_\varepsilon}\right)\frac{\partial \varepsilon}{\partial x_j}\right) - C_{\varepsilon 2}\frac{\varepsilon^2}{k}. \quad (5)$$

The various empirical constants of the model are as follows [24]:

$$C_\mu = 0.09,\ C_{\varepsilon 1} = 1.44,\ C_{\varepsilon 2} = 1.92,\ Pr_k = 1.0,\ Pr_\varepsilon = 1.3,\ \mu_{\mathrm{eff}} = \mu_{\mathrm{nf}} + \mu_{\mathrm{t}}. \quad (6)$$

Boundary conditions

This study involves a temperature labeled $T_{1,in} = 333$ K and a velocity which varies according to the Reynolds number were imposed at the inlet of the inside tube where

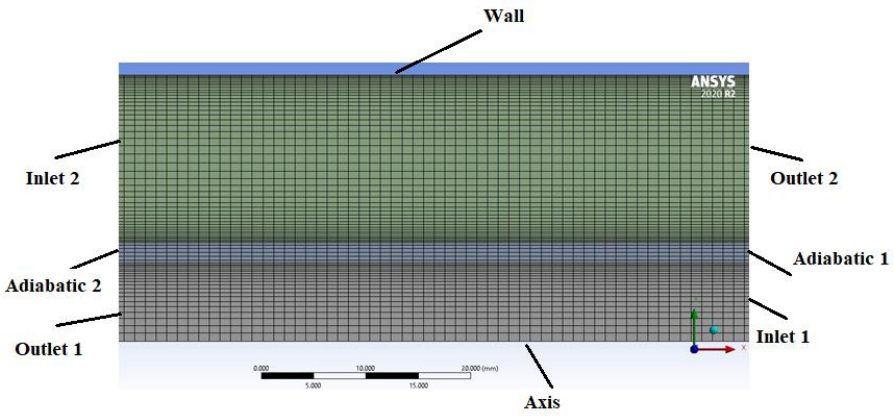

Fig. 2. The heat exchanger mesh and the naming of the boundaries

the hot fluid circulates while at the inlet of the outside tube, the cold fluid enters at a temperature of $T_{0,in} = 293$ K and a velocity which varies according to the Reynolds number. The mesh and the boundaries of the heat exchanger are illustrated in Fig. 2.

The other boundary conditions are as follows: $k = k_{in}$, $k_{in} = \frac{3}{2}(\overline{\mathrm{U}}_{\mathrm{in}}\mathrm{I})^2$, $\varepsilon = \varepsilon_{in}$, $\varepsilon_{in} = C_\mu^{3/4}\frac{k^{3/2}}{\mathrm{L}}$, $L = D_h$ and the turbulent intensity is $I = \frac{u'}{\bar{U}_{mean}} \cdot 100\% = 0.16\left(R_{e_{D_h}}\right)^{-1/8}$, where $\bar{P}_{out,h}$ is the hot fluid outlet, $\bar{P}_{out,c}$ is the cold fluid outlet, and the exterior wall is adiabatic. Interior and exterior walls of the copper tube (fluid-solid interfaces). Right side wall (adiabatic 1) and left side wall of the copper tube (adiabatic 2) are adiabatic.

Nanofluid properties models

The density [25], specific heat [26], thermal conductivity [27], and dynamic viscosity of the nanofluid [28] were calculated using the thermo-physical properties of water and nanoparticles measured on the inlet temperature $\bar{T}$ = 293 K.

In the formulas that follow, the indices (*p*, *f*, and *nf*) correspond to particles, base fluid, and nanofluid, respectively.

Density is:

$$\rho_{nf} = (1-\varphi)\rho_f + \varphi\rho_s. \tag{7}$$

Specific heat is:

$$\left(\rho C_p\right)_{nf} = (1-\varphi)\left(\rho C_p\right)_f + \varphi\left(\rho C_p\right)_s. \tag{8}$$

Thermal conductivity is:

$$\frac{K_{nf}}{K_f} = \frac{K_s+(n-1)K_f-(n-1)(K_f-K_s)\varphi}{K_s+(n-1)K_f+(K_f-K_s)\varphi}. \tag{9}$$

The empirical shape factor φ is expressed as 3Ψ, where Ψ denotes the sphericity, $n = 1$ for spherical nanoparticles, $n = 6$ for cylindrical nanoparticles.

Dynamic viscosity is:

$$\mu_{nf} = \mu_f\,(123\varphi^2 + 7.3\varphi + 1). \tag{10}$$

Principal factors of the problem

This issue of forced convection heat transfer of a nanofluid in fully developed flow can be described by a range of parameters that impact heat transfer and fluid movement within the double-tube counter-current flow heat exchanger, specifically: Prandtl number is $P_{r_{nf}} = \mu_{nf}.C_{p_{nf}}/k_{nf} = \nu_{nf}/\alpha_{nf}$, Reynolds number is $R\mathrm{e} = \frac{\rho_{nf}\bar{V}D_h}{\mu_{nf}}$, which ranges from 10000 to 50000; the nanoparticle volume fraction within the nanofluid was maintained at 30 %, while the hydraulic diameter was determined using the following formula: $D_h = \frac{4A}{P}$.

Heat transfer is quantified by the Nusselt number, which is calculated using the following formula:

$$Nu = \frac{hD_h}{K_{nf}}. \tag{11}$$

For forced convective heat transfer (in case of plane flow) $N_u = 0.66 \cdot pr^{\frac{1}{3}} \cdot Re^{\frac{1}{2}}$, $R_e < R_{ec}$ in laminar flow and $Nu = 0.036 \cdot pr^{\frac{1}{3}} \cdot Re^{\frac{4}{5}}$, $R_e > R_{ec}$ in turbulent flow.

The Nusselt number average $\overline{Nu} = \frac{\bar{h}.D_h}{k_{nf}}$ and the mean heat transfer coefficient $\bar{h} = k_{nf} \times \overline{Nu}/D_h$ are an indicator of the effectiveness of heat transfer between the two fluids.

The friction coefficient utilized is based on the formulation introduced by Haaland [29], which provides an explicit approximation of the Colebrook-White equation:

$$\frac{1}{\sqrt{f}} = -1.8 \log\left[\left(\frac{\frac{\epsilon}{D_h}}{3.7}\right)^{1.11} + \frac{6.9}{R_e}\right]. \quad (12)$$

The formula for the pressure loss is as follows:

$$\Delta\bar{P} = f \frac{L}{D_h} \frac{\rho_{nf} U^2}{2}. \quad (13)$$

The heat transfer rate (Q) in a double tube heat exchanger can be calculated by following formula [30]:

$$Q = U\, A\, LMTD = \dot{m} C_p \Delta\bar{T}, \quad (14)$$

where $\Delta\bar{T} = \bar{T}_{out} - \bar{T}_{in}$ indicates the variation in temperature of the fluid between the inlet and outlet.

The goal of this numerical study is to evaluate the impact of the Reynolds number and the chosen heat transfer fluid on the flow dynamics and heat transfer within a double-tube exchanger used to cool hot water to 333 K. Two fluids were used: water and the nanofluid water / Al_2O_3. The numerical results obtained using Ansys Fluent software 2020 R2 were graphically represented and discussed. The plotted graphs show the temperature fields, the pressure fields as well as the friction factor, the total exchange coefficient, the rate of heat transfer and the mean Nusselt number following the streamlines of the exchanger for a Reynolds number of 20000, of both cases cold water and nanofluid.

Simulation method

This numerical study utilizes the finite volume method S. Patankar [31] to solve the equations embedded in the commercial code Ansys Fluent software 2020 R2. The methods used are: The pressure field is determined using SIMPLE (Semi-Implicit Method for Pressure-Linked Equations), while the convection term in the governing equations is approximated with an upstream second-order scheme. The resulting systems of algebraic equations are solved using a line-by-line procedure alongside the Gauss-Seidel iterative technique convergence of the solution is achieved as the normed residual of every algebraic equation falls below 10^{-4} for the continuity equations and momentum, yet below 10^{-6} for the energy equation.

Results and commentary

Code validation

The computational code was validated by contrasting the computed pressure drop results against the analytical ones (see Fig. 3 and 4). The analytical values of the pressure drop were obtained from Eq. (12) for heat transfer in turbulent forced convection involving hot and cold water. The present numerical predictions closely match the analytical values, with differences so negligible that the results appear virtually the same.

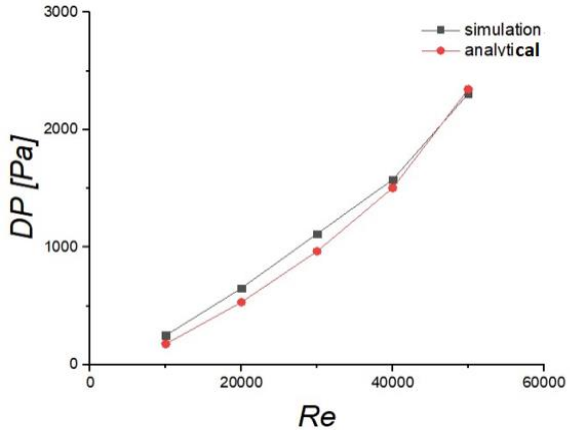

Fig. 3. Comparison of pressure loss between simulated and analytical results of the hot fluid as function of Reynolds number

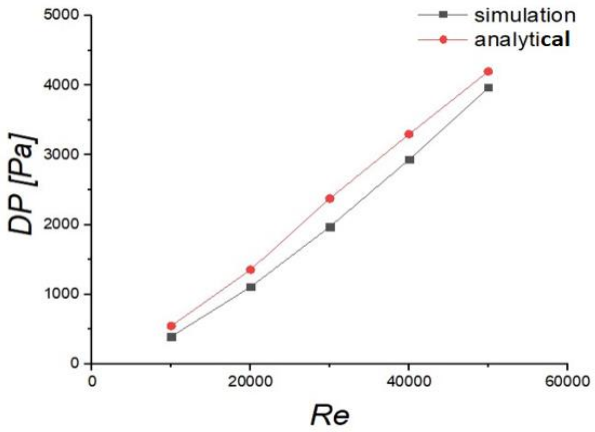

Fig. 4. Comparison of pressure loss between simulated and analytical results of the cold fluid as function of Reynolds number

Thermal field

Figures 5 and 6 present the temperature contours in an r-z plane along the exchanger. It is observed that, in the case where cold water is present in the outer tube, the thermal distribution within the inner tube reveals that the hot water has a high temperature, thus indicating a transfer of heat from the inside towards the outside. The temperature gradually decreases along the inner tube due to heat exchange with the cold water in the outer tube whose temperature gradually increases along the tube. When the nanofluid flows into the outside tube, the temperature decreases faster along the heated tube, and the temperature of the nanofluid gradually increases along the tube. This enhancement

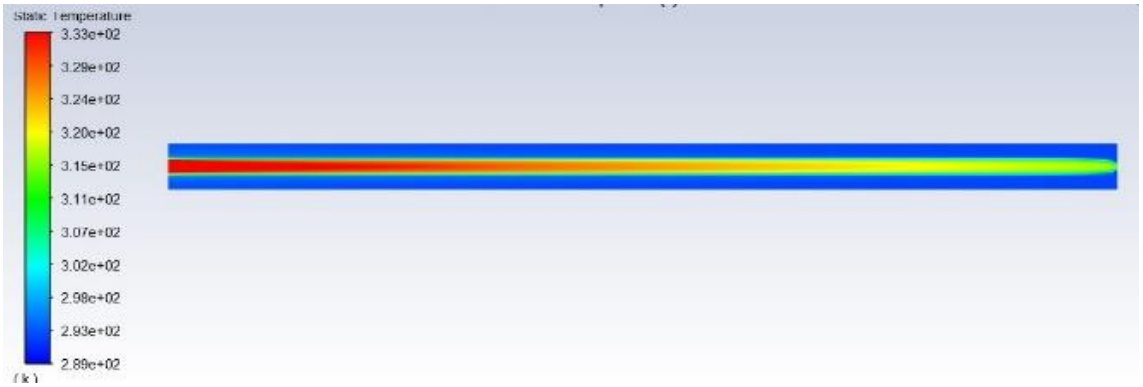

Fig. 5. Temperature contours in a r-z plane, for Reynolds number of 20000 when using cold water

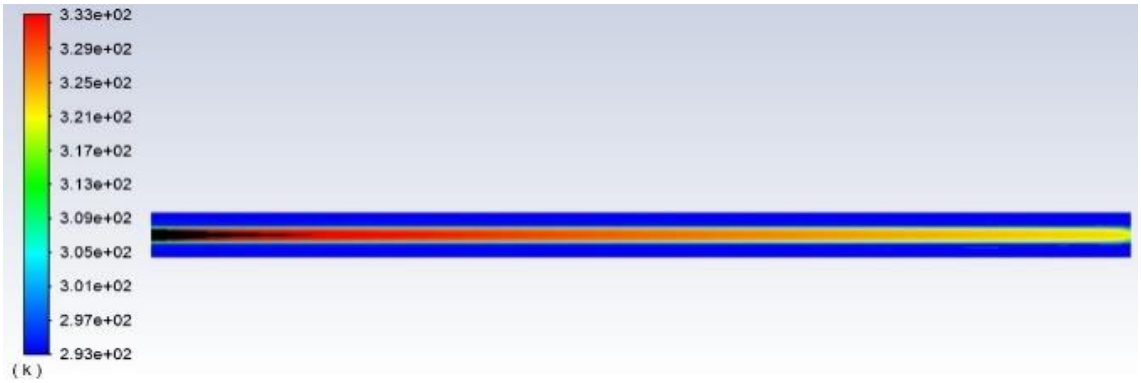

Fig. 6. Temperature contours in a r-z plane, for Reynolds number of 20000 when using nanofluid

is more evident than with cold water, attributable to the nanofluid's excellent thermal conductivity. Differences in heat performance between the two cases can also be observed through the distribution and variation of temperatures along the heat exchanger.

Figure 7 shows the variation in the temperature of the hot water at the exit of the inner tube. When cold water is utilized in the outer tube, the hot water temperature is expected to be higher at the end of the inner tube due to the low overall exchange coefficient. In contrast, when the nanofluid is used in the outer tube, the high thermal conductivity can improve the heat exchange efficiency by increasing the *U* value, resulting in more efficient cooling of the hot water at the outlet of the internal tube.

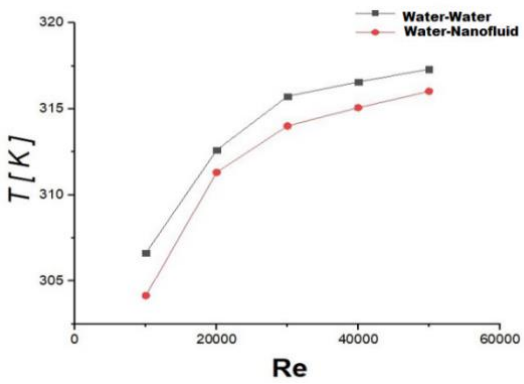

Fig. 7. Temperature variation of the hot water at the outlet of the inner tube with respect to the Reynolds number in both cases

However, a decrease in the cooling rate of hot water can occur with increasing Reynolds number, due to increased flow rates of the fluid passing through the exchanger. This conclusion can be drawn using the formula for the quantity of heat exchanged, which is: $\mathrm{Q} = \mathrm{U\ A\ LMTD} = \dot{m}\ C_p\ \Delta\bar{T}$. Thus, we can see from Fig. 7 that $\Delta\bar{T}_{Re=10000} > \Delta\bar{T}_{Re=20000} > \Delta\bar{T}_{Re=30000} > \Delta\bar{T}_{Re=40000} > \Delta\bar{T}_{Re=50000}$.

Flow field

Figures 8 and 9 reflect the changes in the flow of dynamics along the heat exchanger. It can be noticed from these figures that, in the case where cold water is present in the outer tube, the contour of the stream function shows a lower maximum value than in

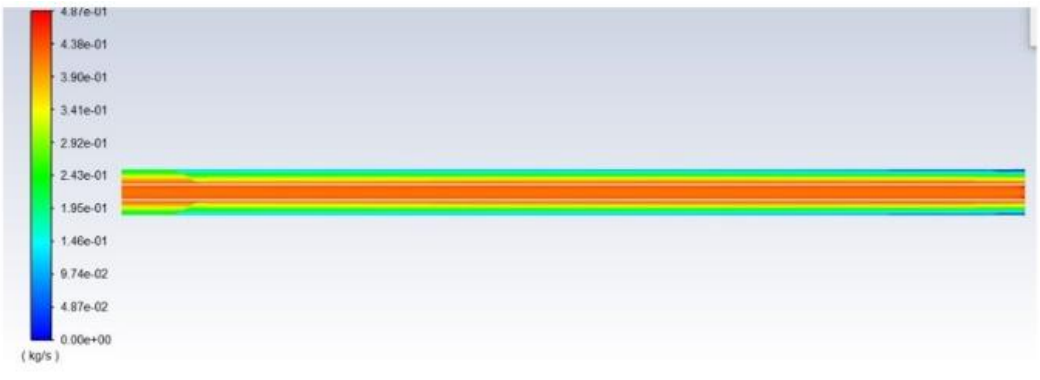

Fig. 8. Contours of the stream function ψ (kg/s) in an r-z plane along the exchanger for Reynolds number of 20000, for the water-water exchanger

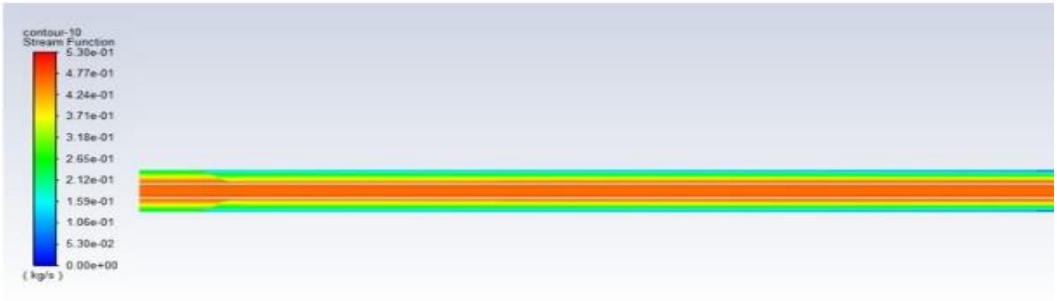

Fig. 9. Contours of the stream function ψ (kg/s) in an r-z plane along the exchanger for Reynolds number of 20000, for the nanofluid-water exchanger

the case of the nanofluid. This is because of the nanofluid's density which is higher than that of water. Indeed, the value of the stream function is given by the formula:

$$\psi = \psi_0 + \rho \int_{y_p}^{y=0} Urdr \text{ with } \psi_0 = 0 \quad (15)$$

These figures also indicate that the velocity profile changes along the inner tube from a uniform profile at the inlet ($\bar{U} = \bar{U}_{1,in}, \bar{V} = 0$) towards a profile developed at a distance $\mathrm{Z} = 4.4.\mathrm{Re}^{1/6} = 22.92,\ \mathrm{D} = 344\ \mathrm{mm}$ from the entrance. Beyond this value the profile remains constant $\left(\frac{\partial \bar{U}}{\partial z} = \frac{\partial \bar{V}}{\partial z} = 0\right)$. However, the velocity profile along the outer annular pipe changes from a uniform profile at the inlet ($\bar{U} = \bar{U}_{0,in},\ \bar{V} = 0$) but does not reach the developed state.

Pressure fields reach

Figure 10 presents the pressure contours for the case where cold-water flows in the outer tube. The results show a maximum pressure drop ($\Delta\bar{P}$) of 5.34 Pa across the two tubes. In contrast, Fig. 11 illustrates the case of nanofluid circulating in the outer tube, where the maximum pressure drops ($\Delta\bar{P}$) reaches 454 Pa. This indicates that the pressure loss due in the case of the nanofluid, the heat exchanger shows increased performance which implies greater pumping power when used as a cooling fluid. The cause of this difference is the high viscosity of the nanofluid, which leads to: $\tau_{p\ \text{nanofluid}} = 8.356 > \tau_{p\ \text{cold water}} = 5.92$.

Fig. 10. Pressure contours in an r-z plane along the exchanger for a Reynolds number of 20000 for the water-water exchanger

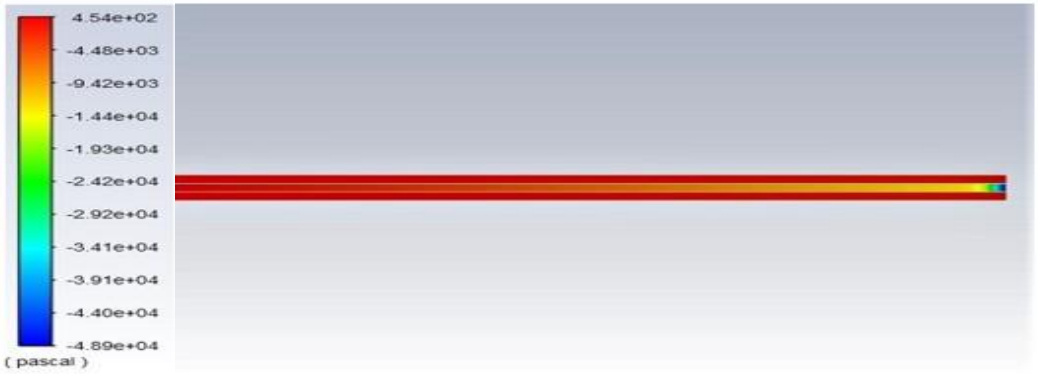

Fig. 11. Pressure contours in an r-z plane along the exchanger for a Reynolds number of 20000, for the nanofluid-water exchanger

Overall heat exchange coefficient

Figure 12 illustrates the change in the total heat transfer coefficient (*U*) along the tube. When using the nano fluid within the outer tube, an increase in the coefficient of total heat transfer is measured over the entire Reynolds number range compared with cold water. This indicates increased efficiency in heat transfer through the heat exchanger when using the nano fluid.

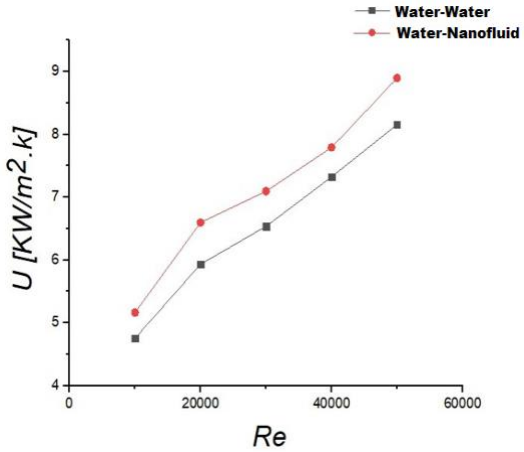

Fig. 12. Variation t of the total heat transfer coefficient *U* throughout the tube *U* as a function of the Reynolds number in both cases

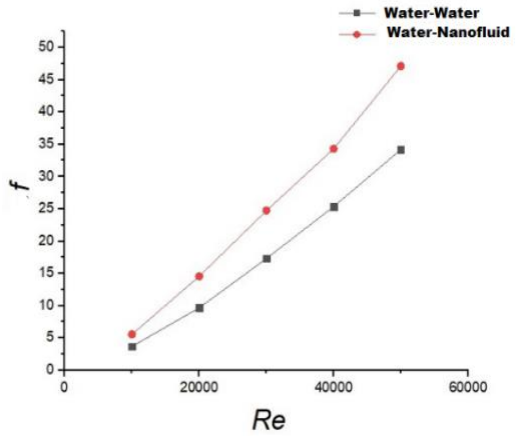

Fig. 13. Variation of the friction coefficient (*f*) with respect to the Reynolds number in both cases

Friction coefficient

Figure 13 presents the change in the friction coefficient ƒ throughout the tube. A rise in the friction coefficient is noted when utilizing the nanofluid compared to cold water for the entire Reynolds number range. This increase can be linked to the increased value of the viscosity of the nanofluid in comparison with that of water. Indeed, high viscosity results in greater resistance τ to the flow.

Rate of heat transfer

The curves in Fig. 14 indicate an improvement in the heat transfer rate when employing a nanofluid compared to cold water for the entire range of Reynolds numbers. This is due to the increase in coefficient of convective exchange as a function a Reynolds number. Raising the number of Reynolds signifies higher velocities close to the fluid-copper wall interfaces, which promotes convective heat transfer across these interfaces.

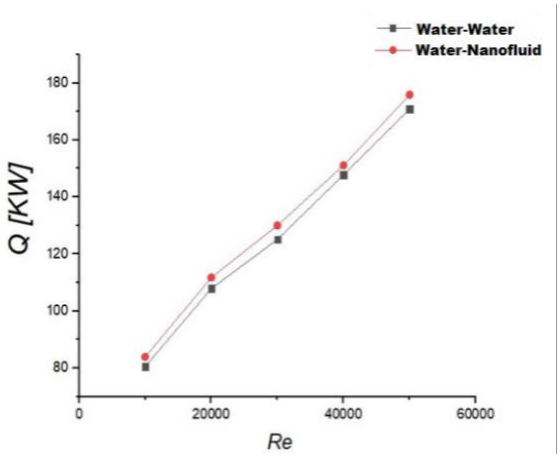

Fig. 14. Variation of the heat transfer rate Q in relation to the Reynolds number in both cases

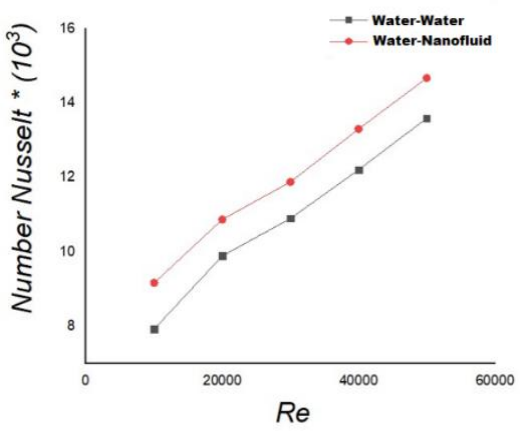

Fig. 15. Variation of the Nusselt number as a function of the Reynolds number in both cases

Nusselt number

Figure 15 illustrates the change in the Nusselt number Nu at the hot fluid-copper wall interface. When using the nano fluid in the outer tube an increase in the Nusselt number across the scale of Reynolds numbers is observed compared to cold water. One can also note from Fig. 15 that the difference between the Nusselt numbers for the water-water and the water-nanofluid exchangers remains constant as the Reynolds number rises.

Conclusions

The numerical investigation of flow and heat transfer in a double-tube heat exchanger was carried out considering the impact of the Reynolds number and the fluid type on temperature of the hot water, on the total convective exchange coefficient, on the friction coefficient, on the rate of heat transfer and its Nusselt number. The ANSYS-Fluent 2020.R2 calculation code was employed to solve the transport equations.

The aim of this study is to compare the nano fluid and cold water in terms of performance which is measured by the performance of the heat exchanger and the pressure drop within it.

Key findings from this study are summarized as follows:

1. An increase in Reynolds' number produces a significantly higher transfer rate.
2. The best improvement in the performance of the heat exchanger was obtained by using the nanofluid.
3. The friction coefficient is greater for the nanofluid

CRediT authorship contribution statement

Rabah Nebbati: writing – review & editing, writing – original draft, conceptualization, investigation, supervision, data curation; **Mahfoud Kadja**: writing – review & editing, writing – original draft, conceptualization, supervision; **Farid Mechighel**: writing – review & editing, investigation.

Conflict of interest

The authors declare that they have no conflict of interest.

References

1. Bergman TL, Lavine AS, Incropera FP, DeWitt DP. *Fundamentals of Heat and Mass Transfer.* New York: John Wiley & Sons; 1996.
2. Cengel YA, Boles MA. *Thermodynamics: An Engineering Approach.* New York: McGraw-Hill; 2002.
3. Shah RK, Sekulić DP. *Fundamentals of Heat Exchanger Design.* Hoboken (NJ): John Wiley & Sons; 2003.
4. Kakaç S, Liu H, Pramuanjaroenkij A. *Heat Exchangers: Selection, Rating, and Thermal Design.* Boca Raton (FL): CRC Press; 2002.
5. Bejan A. *Advanced Engineering Thermodynamics.* Hoboken (NJ): John Wiley & Sons; 2016.
6. Pathak R, Geete A. Thermal performance analyses of concentric pipe counter flow heat exchanger at different operating conditions by CFD. *i-Manager's Journal on Mechanical Engineering.* 2019;9(1): 1–12.
7. Choi SUS. Enhancing thermal conductivity of fluids with nanoparticles. In: *1995 ASME International Mechanical Engineering Congress and Exposition: Proceedings of the ASME Materials Division, 12–17 November 1995, San Francisco, California.* New York: American Society of Mechanical Engineers; 1995. p.95–105.
8. Mousavi M, Darvishi P, Pouranfard A. Comparative study of heat transfer and pressure drop in turbulent flow of a singular and hybrid nanofluids into a horizontal pipe. *Journal of Thermal Analysis and Calorimetry.* 2023;148:14375–14384.
9. Ali S, Krishna K, Reddy S, Ali S. Thermal analysis of double pipe heat exchanger by changing the materials using CFD. *International Journal of Engineering Trends and Technology.* 2015;26(2): 95–102.
10. Dhoria SH, Kumar EM, Yeswanth IVS, Jayanti L. CFD analysis on concentric tube heat exchanger in parallel and counter flow direction. *International Journal of Engineering Research and Applications.* 2018;8(6): 20–25.
11. Ahmed F, Sumon MM, Fuad M, Gugulothu R, Mollah AS. Numerical simulation of heat exchanger for analyzing the performance of parallel and counter flow. *WSEAS Transactions on Heat and Mass Transfer.* 2021;16: 145–152.
12. Darzi AAR, Farhadi M, Sedighi K. Heat transfer and flow characteristics of Al_2O_3–water nanofluid in a double tube heat exchanger. *International Communications in Heat and Mass Transfer.* 2013;47: 105–112.
13. Tavousi E, Perera N, Flynn D, Hasan R. Heat transfer and fluid flow characteristics of the passive method in double tube heat exchangers: a critical review. *International Journal of Thermofluids.* 2023;17: 100282.
14. Naphon P. Heat transfer and pressure drop in the horizontal double pipes with and without twisted tape insert. *International Communications in Heat and Mass Transfer.* 2006;33(2): 166–175.
15. Córcoles JI, Moya-Rico JD, Molina A, Almendros-Ibáñez JA. Numerical and experimental study of the heat transfer process in a double pipe heat exchanger with inner corrugated tubes. *International Journal of Thermal Sciences.* 2020;158: 106526.
16. Chun B-H, Kang H-U, Kim S-H. Effect of alumina nanoparticles in the fluid on heat transfer in double-pipe heat exchanger system. *Korean Journal of Chemical Engineering.* 2008;25: 966–971.
17. Mansoury D, Ilami Doshmanziari F, Kiani A, Chamkha AJ, Sharifpur M. Heat transfer and flow characteristics of Al_2O_3/water nanofluid in various heat exchangers: experiments on counter flow. *Heat Transfer Engineering.* 2020;41(3): 220–234.
18. Dharmalingam R, Sivagnanaprabhu KK, Yogaraja J, Gunasekaran S, Mohan R. Experimental investigation of heat transfer characteristics of nanofluid using parallel flow, counter flow and shell and tube heat exchanger. *Archive of Mechanical Engineering.* 2015;62(4): 509–522.
19. Zarringhalam M, Karimipour A, Toghraie D. Experimental study of the effect of solid volume fraction and Reynolds number on heat transfer coefficient and pressure drop of CuO–water nanofluid. *Experimental Thermal and Fluid Science.* 2016;76: 342–351.

20. Braga CVM, Saboya FEM. Turbulent heat transfer, pressure drop and fin efficiency in annular regions with continuous longitudinal rectangular fins. *Experimental Thermal and Fluid Science.* 1999;20(2): 55–65.
21. Bouazizi L, Turki S. Combined effects of viscous dissipation and Brownian motion on temperature distribution and heat transfer of Al_2O_3/water nanofluid flow through a porous medium. *Materials Physics and Mechanics.* 2021;47(6): 921–936.
22. Pulin AG, Laptev MA, Alisov KA, Barskov VV, Rassokhin VA, Gong B, Kotov VS, Roshchenko GA, Balakin AM, Golubtsov M, Nurkov IR, Basati Panah M. Heat exchanger and the influence of lattice structures on its strength. *Materials Physics and Mechanics.* 2024;52(6): 61–80.
23. Taourit F. Étude du comportement dynamique et thermique de deux écoulements du fluide dans un échangeur de chaleur (comparaison entre le cas simple et le cas avec ailettes). *Université Abou Bekr Belkaïd Tlemcen.* Tlemcen (Algeria): Mémoire de master (option génie énergétique); 2013.
24. Launder BE, Spalding DB. The numerical computation of turbulent flows. *Computer Methods in Applied Mechanics and Engineering.* 1974;3(2): 269–289.
25. Pak BC, Cho YI. Hydrodynamic and heat transfer study of dispersed fluids with submicron metallic oxide particles. *Experimental Heat Transfer.* 1998;11(2): 151–170.
26. Xuan Y, Roetzel W. Conceptions for heat transfer correlation of nanofluids. *International Journal of Heat and Mass Transfer.* 2000;43(19): 3701–3707.
27. Hamilton RL, Crosser OK. Thermal conductivity of heterogeneous two-component systems. *Industrial & Engineering Chemistry Fundamentals.* 1962;1(3): 187–191.
28. Maiga SEB, Palm SJ, Nguyen CT, Roy G, Galanis N. Heat transfer enhancement by using nanofluids in forced convection flows. *International Journal of Heat and Fluid Flow.* 2005;26(4): 530–546.
29. Haaland SE. Simple and explicit formulas for the friction factor in turbulent pipe flow. *Journal of Fluids Engineering.* 1983;105(1): 89–90.
30. Kakaç S, Liu H, Pramuanjaroenkij A. *Heat Exchangers: Selection, Rating, and Thermal Design.* 3rd ed. Boca Raton (FL): CRC Press; 2012.
31. Patankar SV. *Numerical Heat Transfer and Fluid Flow.* New York: McGraw-Hill; 1980.